Time-differential perturbed-angular-correlation studies of radiation damage with radioactive probes implanted in cubic metals

H. G. Müller, K. Krien, and E. Bodenstedt
Institut für Strahlen- und Kernphysik der Universität Bonn, Germany
(Received 3 August 1976)

The direct "microscopic" study of radiation damage by means of time-differential perturbed-angular-correlation measurements with implanted radioactive probes is shown to be a promising new technique. First results are reported for the fcc metals Cu, Al, and Pt. The radioactive probe ^{111}In was implanted by use of an electromagnetic isotope separator at an energy of 80 keV. The radiation damage studied was that produced by the ion implantation itself. After implantation at 24 K essentially 100% of the probe nuclei experience a distribution of strong electric field gradients due to nearest-neighbor defects. After implantation at 293 K in most cases dominant fractions are influenced by further distant radiation damage. In general, after annealing the interaction patterns changed. In one case (Pt) the measurements revealed the trapping of a single defect by the implanted impurity. This defect-ion pair was destroyed again after annealing at 673 K. The defect is interpreted as a single vacancy.

I. INTRODUCTION

Up until now only a few "microscopic" investigations of the radiation damage in solids have been reported. These investigations used the Mössbauer technique[1] or the perturbation of γ angular distributions after nuclear reactions[2,3] or of γ-γ angular correlations for the observation of hyperfine fields produced by defects in the host lattice around the probe nucleus.[4]

All investigations of this kind can be classified as on-line or off-line experiments. In on-line experiments the hyperfine fields are observed for up to a few hundred nanoseconds after the production of the excited probe nucleus. Annealing processes can be studied by these methods only as far as they happen within this short time interval. Off-line experiments on the other hand allow one to study annealing processes at a larger time scale: here one is only limited by the half-life of the radioactive probe.

A second classification may be done according to the production of the radiation damage. In one group of experiments the bulk material is irradiated by fast neutrons, charged particles or γ rays and the position of the probe nucleus is not correlated with the location of the defects. The extreme alternative is local production of radiation damage by implantation of the probe atom itself. The latter method has from the experimental point of view the advantage that highly damaged sites can be studied without the need of a high radiation dose or long irradiation times. This allows in a fast and economic way studies of radiation damage produced at low temperatures where both the interstitial atoms and the vacancies are not mobile.

In this paper we report on first results of time-differential perturbed-angular-correlation (TDPAC) investigations with radioactive probes which were implanted by an electromagnetic isotope separator into the fcc metals Cu, Al, and Pt at 24 K and at room temperature. The reason for the choice of cubic hosts is simply the fact that probe nuclei in regular sites of undamaged lattices experience no electric field gradient (EFG). Any observed perturbations of the γ-γ angular correlations are therefore due to defects in the lattice produced in this experiment by the ion implantation itself.

II. EXPERIMENTAL PROCEDURE

Commercial Cu, Al, and Pt foils of 99.9-at.% purity and 25-μm thickness were chosen as host materials for the implantations. The oxid layers were removed mechanically and the collection foils then quickly placed into the vacuum of the isotope separator. In our estimate this technique reduces the oxid layer, e.g., for Al to a very few atomic layers only. Implantations and subsequent first TDPAC measurements were carried out with the host lattice kept at 24 K at all times in order to avoid annealing of the produced radiation damage. This was achieved by use of a liquid-He cryostat, which could be attached via a short beam pipe to the isotope separator to perform the implantation into the cold host lattice. A cold trap in this beam pipe was to stop oil vapors from the diffusion pumps of the isotope separator from reaching the ion beam collecting foils. The ion implantations were carried out at acceleration voltages of 80 kV and ion beam currents of about 10 μA. The total dose of implanted ions ranged between 5×10^{13} and 1×10^{15}

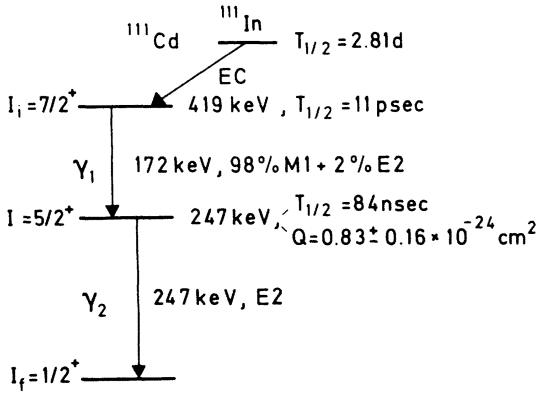

FIG. 1. Partial decay scheme of ^{111}In-^{111}Cd.

ions/cm^2. This corresponds to average impurity concentrations between 0.02 and 0.8 at.%. According to the Lindhard theory,[5,6] the most probable penetration depth of the implanted ^{111}In ions at this energy is about 55 atom layers for Pt, 80 atom layers for Cu, and 170 atom layers for Al. Strong influences of surface effects on our TDPAC measurements are therefore not to be expected. In order to perform the TDPAC experiments a vacuum valve at the cryostat was closed so that the cryostat could be moved to the angular-correlation apparatus for an initial measurement with the sample at 24 K. Lower sample temperatures could not be reached because of the heat radiation through the ion beam entrance opening in the liquid-N_2 shield. The samples were then isochronally tempered for 30 min at progressively higher temperatures with a TDPAC measurement after each annealing step. Annealing at temperatures below 293 K was carried out under vacuum inside the cryostate using an internal heating device. At higher temperatures the samples were transfered into small evacuated tubes of quartz being sealed before annealing. For comparison implantations were performed also at 293 K and the samples then treated in the same way. The implanted radioactivity ^{111}In was obtained from New England Nuclear. For the TDPAC measurements the 172–247-keV $\gamma\gamma$ cascade in the decay product ^{111}Cd (see Fig. 1) was used. The conventional angular correlation apparatus consisted of two NaI(Tl) detectors and standard fast-slow electronics. The time resolution (full width at half-maximum) varied between 2.2 and 3.6 nsec for different measurements. The detectors were positioned alternately every 1000 sec at angles $\theta = \pi$ and $\theta = \frac{1}{2}\pi$ with respect to each other. The coincidence counting rates $N(\theta, t)$ as a function of the time delay t between the two γ emissions were stored in separate subgroups of a multichannel analyzer.

The observed time spectra exhibit the exponential decay due to the lifetime τ of the intermediate state modulated by the time-dependent angular correlation function $W(\theta, t)$:

$$N(\theta, t) = Ae^{-t/\tau} W(\theta, t). \tag{1}$$

For the case of polycrystalline environment of the nuclei the angular correlation function is theoretically[7] of the form

$$W(\theta, t) = \sum_k A_{kk} G_k(t) P_k(\cos\theta). \tag{2}$$

P_k are the Legendre polynomials and A_{kk} the angular correlation coefficients. For the cascade considered here only A_{22} was found[8] to be nonzero

$$A_{22} = -0.180(2), \quad A_{44} = 0.002(3).$$

$G_k(t)$ accounts for the perturbations due to the hyperfine interactions in the intermediate state of the cascade. In the special case of static quadrupole interactions of the nuclear quadrupole moment Q with an axially symmetric unique electric field gradient (EFG) V_{zz} one has

$$G_k(t) = \sum_n s_{kn} \cos n\omega_0 t \ , \tag{3}$$

with

$$\omega_0 = [3/2I(2I-1)] eQV_{zz}/\hbar \tag{4}$$

for half-integer spin I of the intermediate level. The s_{kn} are geometrical factors which are tabulated for $I = \frac{5}{2}$ in Ref. 9.

One can combine the experimental time spectra to eliminate the exponential decay factor by forming the asymmetry ratio

$$R(t) = 2\,\frac{N(\pi, t) - N(\frac{1}{2}\pi, t)}{N(\pi, t) + N(\frac{1}{2}\pi, t)}\,. \tag{5}$$

Inserting Eqs. (1) and (2), one finds, to a good approximation,

$$R(t) \simeq \tfrac{3}{2} A_{22} G_2(t). \tag{6}$$

III. RESULTS

Some experimental $R(t)$ spectra after implantation at $T_{\text{impl}} = 24$ K and $T_{\text{impl}} = 293$ K are shown in Figs. 2 and 3, respectively. The graphs are labeled by the temperature of the sample during the angular correlation measurement T_{mes} and the maximum annealing temperature T_{anneal} when not identical with T_{mes}. The data have been corrected for finite solid angles of the detectors.

A simple periodic rotation pattern according to Eq. (3) is not observed experimentally. The reason is that the implanted nuclei are not exposed to unique EFG's. Instead distributions of

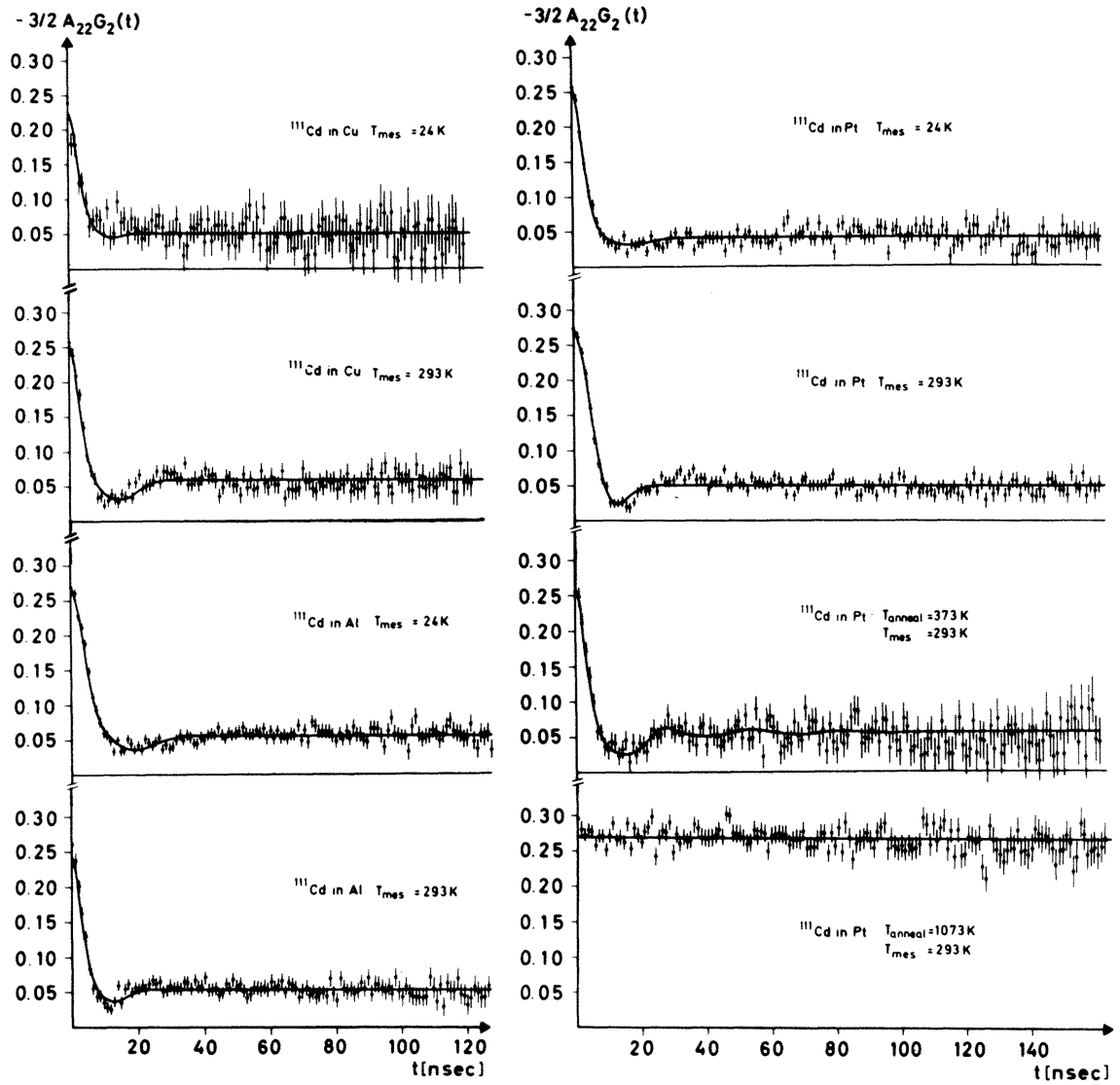

FIG. 2. Results of the TDPAC measurements of ^{111}In-^{111}Cd implanted into fcc metals at 24 K. The graphs are labeled by the host elements, the temperature during the experiment T_{mes} and the annealing temperature, if higher than T_{mes}. The solid lines are least squares fits (see text).

EFG's with relative widths δ around mean values are encountered. This is reflected in similar spreads in interaction frequencies around centroids $\bar{\omega}$. In addition it is not to be expected that the EFG's arise from only one type of defect produced in the host. Accordingly, assuming static quadrupole interaction of axial symmetry, four different contributions to the experimental shapes of the curves were considered:

(i) A broad Gaussian frequency distribution around a high centroid frequency $\bar{\omega}$ in the range of 100–200 MHz corresponding to a distribution of strong EFG's resulting from many defects in the depletion zone of the collision cascade

$$G_2^{(1)}(t) = \sum_n s_{2n} \cos(n\bar{\omega}t) \exp[-\tfrac{1}{2}(\delta n\bar{\omega}t)^2].$$

(ii) A narrow Lorentzian frequency distribution around $\omega_0 \simeq 200$ MHz corresponding to a fraction of nuclei exposed to EFG's due to a unique type of defect at a close distance

$$G_2^{(2)}(t) = \sum_n s_{2n} \cos(n\omega_0 t) \exp(-\tfrac{1}{2}\delta n\omega_0 t).$$

(iii) A broad Gaussian frequency distribution around $\bar{\omega} = 0$ corresponding to a fraction of nuclei experiencing a spread of weak EFG's only due to defects at larger distances

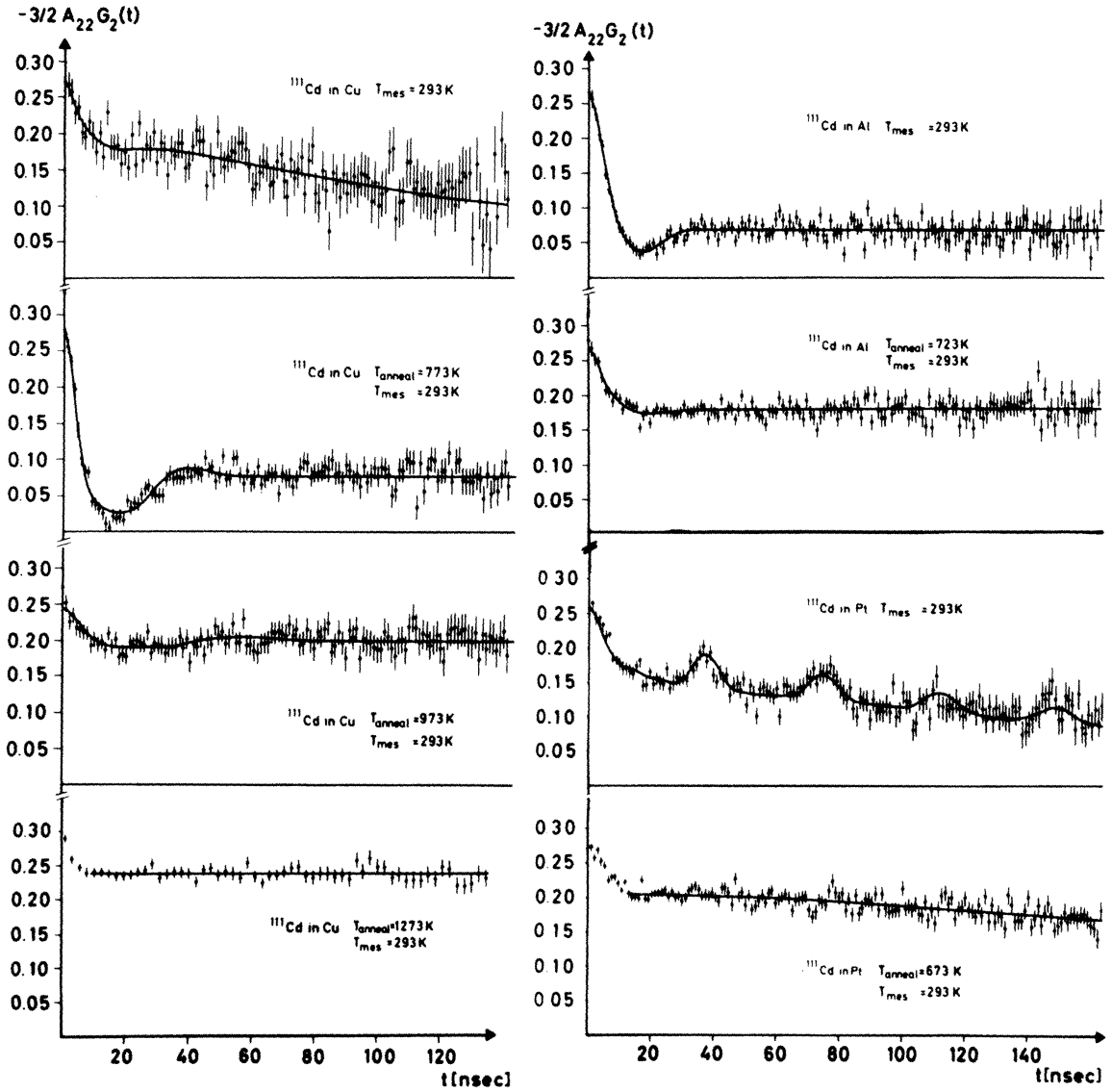

FIG. 3. Same as in Fig. 2, except that the implantation temperature was 293 K.

$$G_2^{(3)}(t) = \sum_n s_{2n} \exp[-\tfrac{1}{2}(\delta_0 n t)^2].$$

(iv) A contribution from nuclei subject to no interaction because they occupy sites of cubic symmetry in an area of undamaged lattice

$$G_2^{(4)}(t) = 1.$$

The solid lines in Figs. 2 and 3 are results of least-squares fits where the perturbation factor was assumed to be a combination of model functions (i)–(iv):

$$G_2(t) = \sum_{i=1}^{4} f_i G_2^{(i)}(t). \tag{7}$$

In all experiments only one or two contributions are dominant so that except for very few cases two or even three of the f_i could be kept zero, which reduced the number of free parameters considerably. Allowance for nonaxially symmetric EFG's did not lead to significantly better agreement between the fitted curves and the data. The finite time resolution was taken into account in the fitting procedures. The derived parameters are summarized in Tables I and II.

IV. DISCUSSION

A. General remarks

Since Cd as well as the host materials are diamagnetic, the observed perturbations of the angular correlation cannot be due to magnetic

TABLE I. Least-squares-fit results of the TDPAC measurements after implantation at 24 K.

Host	T_{anneal} (K)	T_{mes} (K)	Centroid frequency $\bar{\omega}$ (MHz)	Relative spread around $\bar{\omega}$ δ	Amplitude $f_1(\bar{\omega})$	Amplitude f_4
Cu	...	24	166 ±20	0.98 ±0.22	100%	...
Cu	140	24	171 ±8	0.54 ±0.03	100%	...
Cu	...	293	154 ±5	0.59 ±0.03	100%	...
Al	...	24	107 ±2	0.67 ±0.02	100%	...
Al	...	293	163 ±5	0.69 ±0.04	100%	...
Pt	...	24	121 ±12	0.74 ±0.06	100%	...
Pt	...	293	171 ±7	0.73 ±0.03	100%	...
Pt	373	293	149 ±9	0.58 ±0.04	(92 ±5)%[a]	...
Pt	573	293	124 ±23	0.92 ±0.20	97%	3%
Pt	1073	293	...	...	...	100%

[a] In addition there is a $f_2 = (8 \pm 5)\%$ contribution of a frequency $\omega_0 = 222 \pm 14$ MHz with small relative spread $\delta = 0.10 \pm 0.01$.

interactions. For the reasons discussed in Ref. 3, time-dependent interactions are also improbable. For large delay times the experimental asymmetry ratios are in all cases larger than or equal to the hard-core value

$$|\tfrac{3}{2}A_{22}s_{20}| = 0.054$$

expected for static quadrupole interactions with frequency distributions. This justifies the type of functions used in the fits.

According to channeling studies[10] and special computations for an implantation of In into Cu,[11] it is most likely for the implanted nuclei to come to rest on regular lattice sites. But even if some of the ^{111}In-^{111}Cd impurity ions should occupy interstitial sites they would be most probably the octahedral type, which have cubic symmetry also. Therefore, the observed perturbations of the angular correlation must be due to interactions with defects in the neighborhood.

Assuming a point defect at a distance d from the ^{111}Cd nuclei one can estimate the expected interaction frequency ω_0 in the following way using Eq. (4). The quadrupole moment Q of the $I = \frac{5}{2}$ 247-keV state of ^{111}Cd is known[12] to be

$$Q = 0.83 \pm 0.16 \text{ b}.$$

The effective EFG at the ^{111}Cd site is parametrized as

$$V_{zz}^{eff} = NV_{zz}(d)(1 - \gamma_\infty^{Cd})(1 - K).$$

$V_{zz}(d)$ is the EFG of an elementary point charge at a distance d which readily can be calculated. N accounts for the assumed charge of the defect. $(1 - \gamma_\infty^{Cd})$ is the Sternheimer antishielding factor[13] describing the polarization of the atomic shell of the ^{111}Cd impurity. The factor $(1 - K)$ accounts for the electronic contribution to the EFG. In accord with Ref. 14, $K = 3$ was assumed. If the distance is measured in terms of the lattice parameter a, this rough estimate yields for Cd in Pt with $N = 2$:

TABLE II. Least-squares-fit results of the TDPAC measurements after implantation at 293 K.

Host	T_{anneal} (K)	T_{mes} (K)	Centroid frequency $\bar{\omega}$ (MHz)	Relative spread around $\bar{\omega}$ δ	Amplitude $f_1(\bar{\omega})$	Amplitude f_4	Amplitude $f_3(\bar{\omega}=0)$	Spread around $\bar{\omega}=0$ δ_0 (MHz)
Cu	...	293	131 ±24	0.69 ±0.31	(40 ±6)%	...	(60 ±6)%	7 ±1
Cu	573	293	174 ±11	0.60 ±0.06	(84 ±2)%	(16 ±2)%	...	...
Cu	773	293	151 ±3	0.36 ±0.02	(93 ±1)%	(7 ±1)%	...	...
Cu	973	293	110 ±7	0.30 ±0.06	(22 ±2)%	(78 ±2)%	...	...
Cu	1273	293	...	...	≤15%	≥85%	...	...
Al	...	293	134 ±5	0.62 ±0.02	(94 ±1)%	(7 ±1)%	...	...
Al	723	293	108 ±7	0.80 ±0.13	(42 ±2)%	(58 ±2)%	...	...
Pt	...	293	53 ±14	0.67 ±0.49	(21 ±5)%[a]	...	(52 ±8)%	7 ±1
Pt	673	293	...	...	~20%	(29 ±10)%	~50%	4 ±1
Pt	873	293	...	...	~10%	(45 ±3)%	~45%	6 ±1

[a] In addition, there is a $f_2 = (28 \pm 3)\%$ contribution of a frequency $\omega_0 = 198 \pm 2$ MHz with small relative spread $\delta = 0.075 \pm 0.005$.

d	$\frac{1}{2}a$	$a/\sqrt{2}$	a	$2a$
ω_0(MHz)	878	310	110	14

$a/\sqrt{2}$ is the minimum distance for the defect on a regular lattice site. For the Al and Cu hosts, similar values are estimated. The rapid decrease of ω_0 with increasing d according to the r^{-3} dependence of the EFG allows a distinction between defects in the nearest neighborhood and at distances of several lattice parameters.

B. Measurements after implantation at 24 K

The measured high values of the centroid frequencies after implantation at 24 K indicate that the observed perturbations are caused by defects trapped in the nearest neighborhood of the probe nuclei. It is most remarkable that in all cases except after annealing at very high temperatures ~100% of the implanted nuclei are subject to these strong interactions. The broad distributions of interaction frequencies prove that a variety of different defect configurations is encountered. From electrical resistivity measurements[15] it is well known that at 24 K interstitials are already mobile in Pt. In the region of the collision cascade during the implantation process a certain mobility is also to be expected for Al at this temperature but not for Cu. This may explain the larger width δ of the frequency distribution observed for *Cu* ^{111}Cd at 24 K as compared to the other two hosts. After annealing of the *Cu* ^{111}Cd sample at 140 K, where interstitials are highly mobile, δ decreases drastically, which indicates the healing of defect configurations which for Pt and Al had already disappeared at 24 K.

At 293 K for Cu and Al the recovery stage III is reached, where vacancies are assumed to be mobile. No corresponding changes of the perturbation patterns are observed. Therefore one must assume that either no vacancies are produced near the probe nuclei or what seems more likely that they are trapped at the In-Cd impurities with such strong binding energies that they become mobile only at higher temperatures. For experimental reasons only the *Pt* ^{111}Cd sample was further annealed at temperatures above 293 K. After tempering at 373 K, a $(8\pm5)\%$ fraction of the ^{111}Cd nuclei seems to experience a unique EFG. The high spin-rotation frequency $\omega_0 = 222\pm14$ MHz indicates a unique nearest-neighbor defect. Although at this temperature the mobility of vacancies in Pt is still low, this could be the case of a single vacancy trapped by the probe ion.

Annealing at 573 K again increases the width of the frequency distribution. Since at this temperature vacancies are mobile in Pt, the increase in δ could be explained by clustering of vacancies; but clustering of In-Cd impurities themselves might also happen. Finally, after annealing at 1073 K all perturbations disappear.

C. Measurements after implantation at 293 K

The *Al* ^{111}Cd samples show no large differences for the two implantation temperatures. The radiation-damage recovery stages for Al are below 293 K.[15] Therefore, the damage is expected to anneal during the room-temperature implantation process. Experimentally, one finds even after annealing at 723 K, a $(42\pm2)\%$ fraction of probe nuclei experiencing interactions with strong EFG's. Since the solubility of In in Al is low[16] and the implanted In activity was carrier free, this might be explained by a migration of the In ions to grain boundaries.[17]

For Cu and Pt the perturbations measured at 293 K after implantation at 24 K are quite different from those after implantation at 293 K. In the latter cases large fractions [$(60\pm6)\%$ and $(52\pm8)\%$, respectively] are exposed to distributions of weak EFG's only, which indicates that the lattice in their immediate neighborhood is undamaged. Weak EFG's are produced by defects at distances of at least a few atomic layers. One must conclude that the formation of nearest-neighbor defects is somewhat suppressed during the implantation at 293 K although according to Sec. IV B after low-temperature irradiation some nearest-neighbor defect structures are stable up to room temperature. Tempering the irradiated Cu foil at 573 and 773 K led to an increase [$(84\pm2)\%$ and $(93\pm1)\%$, respectively] of the probe nuclei subject to strong EFG distributions. This is difficult to explain by defects characteristic of the host material, since they should have recombined completely. Instead agglomerations of the impurities or migrations to grain boundaries may be assumed. This is supported by the low solubility of In in Cu which is[16] 1.2 at.% above 573 K. At lower temperatures it decreases rapidly. Finally, it is observed that at even higher annealing temperatures an increasing fraction of nuclei is free of hyperfine interactions.

For ^{111}In implanted into Pt at 293 K a second $(21\pm5)\%$ fraction of the probe nuclei shows interaction frequencies around a centroid of 53 ± 14 MHz. A third $(28\pm3)\%$ fraction is subject to a unique interaction frequency $\omega_0 = 198\pm2$ MHz indicating a defect in the nearest neighborhood. This frequency is no longer observed after annealing at 673 K, i.e., slightly above recovery stage III for Pt. The defect is therefore assumed to be a vacancy trapped at the In impurity after the im-

plantation. This unique frequency agrees fairly well with that observed after 373-K annealing of the *Pt* ^{111}Cd probe irradiated at 24 K. After tempering of the Pt foil at 673 and 873 K an increasing fraction of the probe nuclei is found on sites of cubic symmetry while the fraction of ^{111}Cd nuclei experiencing EFG's decreases. Compared to the corresponding measurements in Al and Cu the fraction of nuclei exposed to an interaction with strong EFG's after annealing at high temperatures is rather small.

ACKNOWLEDGMENT

The financial support by the Ministerium für Wissenschaft und Forschung des Landes Nordrhein-Westfalen is gratefully acknowledged.

[1]W. Mansel, G. Vogl, and W. Koch, Phys. Rev. Lett. 31, 359 (1973).
[2]H. Bertschat, H. Haas, and F. Pleiter, Conference on Hyperfine Interactions Studied in Nuclear Reactions and Decay, Uppsala, 1974, Contr. II.8, 1974 (unpublished).
[3]J. Bleck, R. Butt, H. Haas, W. Ribbe, and W. Zeitz, Phys. Rev. Lett. 19, 1371 (1972).
[4]M. Behar and R. M. Steffen, Phys. Rev. C 7, 788 (1973).
[5]J. Lindhard and M. Scharff, Phys. Rev. 124, 128 (1961).
[6]J. Lindhard and M. Scharff, H. E. Schott, Kgl. Danske Videnskab. Mat. Fys. Medd. 33, No. 14 (1963).
[7]H. Frauenfelder and R. M. Steffen, in *α-β-γ-Ray Spectroscopy*, edited by K. Siegbahn (North-Holland, Amsterdam, 1965).
[8]R. M. Steffen, Phys. Rev. 103, 116 (1956).
[9]A. Abragam and R. V. Pound, Phys. Rev. 92, 943 (1953).
[10]J. A. Borders and J. M. Poate, Phys. Rev. B 13, 969 (1976).
[11]P. H. Dederichs *et al.*, Phys. Status Solidi 8, 213 (1965).
[12]R. S. Raghavan, P. Raghavan, and J. H. Friedt, Phys. Rev. Lett. 30, 10 (1973).
[13]F. D. Feiock and W. R. Johnson, Phys. Rev. 187, 39 (1969).
[14]P. Raghavan, E. N. Kaufmann, R. S. Raghavan, E. J. Ansaldo, and R. A. Naumann, Phys. Rev. B 13, 2835 (1976).
[15]W. Schilling *et al.*, *Vacancies and Interstitials in Metals*, edited by A. Seeger, D. Schumacher, W. Schilling, and J. Diehl (North-Holland, Amsterdam, 1970).
[16]M. Hansen, *Constitution of Binary Alloys* (McGraw-Hill, New York, 1958).
[17]E. Bodenstedt, U. Ortabasi, and W. H. Ellis, Phys. Rev. B 6, 2909 (1972).